

Article

The Effects of Filter Capacitors on Cable Ripple at Different Sections of the Wind Farm Based Multi-Terminal DC System

Xiaoyun Rong ^{1,*}, Jonathan K. H. Shek ², D. Ewen Macpherson ² and Phil Mawby ¹

¹ School of Engineering, University of Warwick, Library Rd, Coventry CV4 7AL, UK; p.a.mawby@warwick.ac.uk

² Institute for Energy Systems, School of Engineering, University of Edinburgh, Edinburgh EH9 3JL, UK; j.shek@ed.ac.uk (J.K.H.S.); ewen.macpherson@ed.ac.uk (D.E.M.)

* Correspondence: xiaoyun.rong@warwick.ac.uk

† Current address: School of Engineering, University of Warwick, Library Rd, Coventry CV4 7AL, UK

Abstract: In most DC power systems, power electronic devices can introduce ripple content into the DC grid, where large input ripple currents on the DC link can have a negative influence. Under these circumstances, DC side filters play an important role in the reduction of ripple content. In this paper, based on a full detailed closed loop model of the entire offshore wind farm multi-terminal DC network, the effect of filter capacitors connected at different sections of the system on the limitation of the AC ripple content, particularly in the DC cables, is studied. In contrast to other work on HVDC for offshore wind, where simplified or equivalent circuits are mainly used while concentrating on the power and control system, this study can be regarded as the specific study of filter capacitors operating within a detailed system model. Utilising the advantages of PLECS, which is a highly effective tool in the simulation of power electronic circuits, no small-signal or simplified equivalent models are used in the system, and the entire study is based on detailed and accurate models of the semiconductor elements and transformers, which help to provide more realistic simulation results and a better understanding of the system. Another novel point in this paper is a new concept, relative losses, which is proposed to simplify extensively the calculation of losses in this research. Finally, the size of the filter capacitors at different sections of the system under different situations is suggested.

Keywords: DC side capacitors; DC-DC converter; FFT analysis; relative losses; total harmonic distortion



Citation: Rong, X.; Shek, J.K.H.; Macpherson, D.E.; Mawby, P. The Effects of Filter Capacitors on Cable Ripple at Different Sections of the Wind Farm Based Multi-Terminal DC System. *Energies* **2021**, *14*, 7000. <https://doi.org/10.3390/en14217000>

Academic Editors: Anca D. Hansen, Tuhfe Göçmen, Elisabetta Tedeschi, Anne Blavette and Qing Xiao

Received: 27 August 2021

Accepted: 20 October 2021

Published: 26 October 2021

Publisher's Note: MDPI stays neutral with regard to jurisdictional claims in published maps and institutional affiliations.



Copyright: © 2021 by the authors. Licensee MDPI, Basel, Switzerland. This article is an open access article distributed under the terms and conditions of the Creative Commons Attribution (CC BY) license (<https://creativecommons.org/licenses/by/4.0/>).

1. Introduction

Due to the abundance of wind power, its exploitation in the far offshore environment to generate electricity is an attractive topic among researchers. At present, most of the electricity generated from wind power is transmitted via AC systems; however, a DC network has greater advantages for long distance transmission [1]. In the study of offshore wind farm based DC systems, the DC voltage at various sections of the system can be different; this means that DC-DC converters, in a similar way to transformers in an AC system, are essential in the building and development of DC systems. However, as DC-DC converters can introduce much higher harmonics compared with the traditional 12-pulse bridge based DC link, the study of the DC side filter capacitors is important: more so than in a standard 12-pulse bridge based multi-terminal DC system.

The DC side capacitors play an important role to act as an energy buffer to stabilise the DC link voltage and reduce the ripple content. Bulk capacitors can help to reduce the ripple content efficiently, at the cost of larger size and increased cost, as well as reduced reliability because of their short lifetime [2,3]. Reviewing previous related studies, in [3], a control method was developed to reduce the DC-side current ripple in a two-stage single phase inverter, without the need for an auxiliary circuit. In [4], based on an accurate averaging equivalent circuit method, a virtual reactor control strategy was proposed to reduce the size of large fixed reactors on MMCs and the oscillation and instability issue caused by it.

In [5], the interaction between capacitor voltage ripple on the sub-module and the external circuit of a HVDC MMC was established using an enhanced control method. In [6], a novel method was proposed to detect faults in high voltage DC filter capacitors, with high adaptability for different types of faults. In [7], by including series capacitors into the AC filterless LCC point-to-point HVDC system, the active power transfer during a fault was increased significantly.

From [3–7], it is clear that in most of the previous studies, the control method is the key point and the research is typically based on a single converter or a simplified DC system. This paper uses a detailed offshore wind farm based multi-terminal DC system which includes a full closed-loop control circuit at the first stage; the research focuses on the variation in cable ripple content due to the value of filters at different sections of the system, under the same wind speed. Another point is this study is that it also focuses on the AC ripple content, particularly in the DC cables at different sections of the system, which, although important, is less common in existing studies. What is more, in order to simplify the calculation of losses and provide visual data graphically, a new concept, relative losses, is proposed for the first time.

The main contributions of this paper are:

1. The proposed use of multiple and different DC-DC converters to step up the voltage in a multi-connected offshore DC grid is a new solution to collect power from a large offshore wind farm;
2. Investigation of requirements for filters at different sections of the multi-connected system to limit the DC voltage ripple content and AC losses on DC cables;
3. The proposal and definition of the concept of relative AC losses and presentation of an AC efficiency study on multi-connected DC cables;
4. The development of a simplified and downscaled hardware model of the system to verify the effect of filter capacitors at different sections of the system.

2. Structure and Definition of the Offshore Wind Farm Based Multi-Terminal DC System

2.1. Introduction of the Power System

Figure 1 shows a simplified diagram of the wind power system studied in this paper. In the system, a wind turbine with a Permanent Magnet Synchronous Generator (PMSG) captures power from the wind environment and converts it into AC electrical power. A PWM rectifier is used to convert AC power into DC and is subsequently stepped up in voltage with a DC-DC converter. The wind turbine, PMSG, PWM rectifier and the DC-DC converter comprises a sub-block in the system, shown in Figure 1. In the real system, according to the number of wind turbines in the wind farm, there can be hundreds of such sub-blocks connected to the short subsea cables (50 kV cable in Figure 1). An Input Series Input Parallel Output Series (ISIPOS) DC-DC converter can be used to accumulate power from each of the turbines before transmitting to shore via long distance HVDC cables. In this paper, the effectiveness of the filter capacitors, connected at the output of the DC-DC converter in the sub-block and at the input of the ISIPOS DC-DC converter, on reducing ripple content is studied.

For system modelling and simulation, it is impractical and resource intensive to have hundreds of sub-blocks with detailed models and their control circuits at each section of the system, let alone in the hardware testing. Instead, a 15 MW system with three sub-blocks connected onto a single 50 kV cable shown in Figure 2 was modelled to evaluate the effect of the filter capacitors. The reduction of the number of sub-blocks does not influence the property of the filter capacitors at different positions, while the use of an Input Parallel Output Series (IPOS) converter can also reflect the performance of the ISIPOS converter in the system [8].

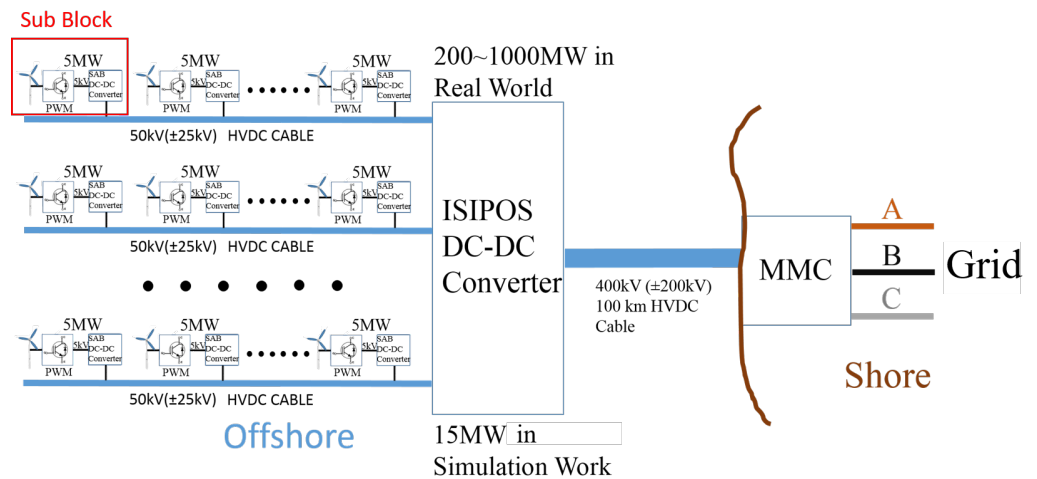


Figure 1. Simplified diagram of the multi-connected system.

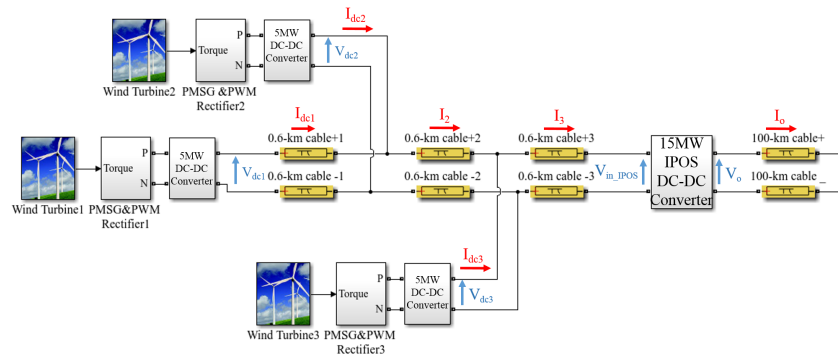


Figure 2. Sending end circuit diagram of a 15 MW wind farm based multi-terminal DC system.

Figures 3 and 4 show the circuit diagram of the 5 MW DC-DC converter and three different structures for a 15 MW IPOS DC-DC converter, respectively. The study of the converters themselves is detailed in [8,9]. In the system model, different values of the output capacitors of the 5 MW DC-DC converters (C_o in Figure 3) and of the input capacitors of the IPOS converters in Figure 4 are simulated to monitor their effects on the ripple content of the voltages and AC losses caused by the ripple content of currents in the multi-connected section of the system.

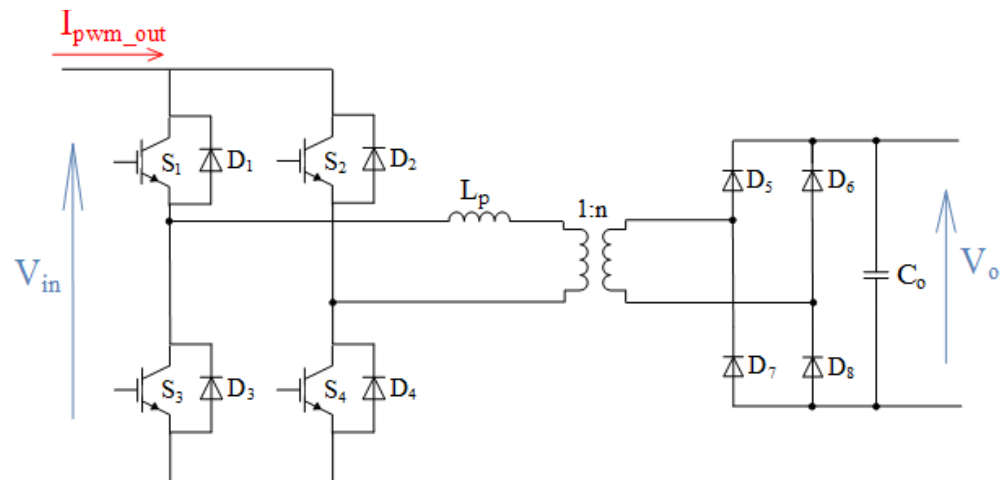


Figure 3. Single active bridge converter.

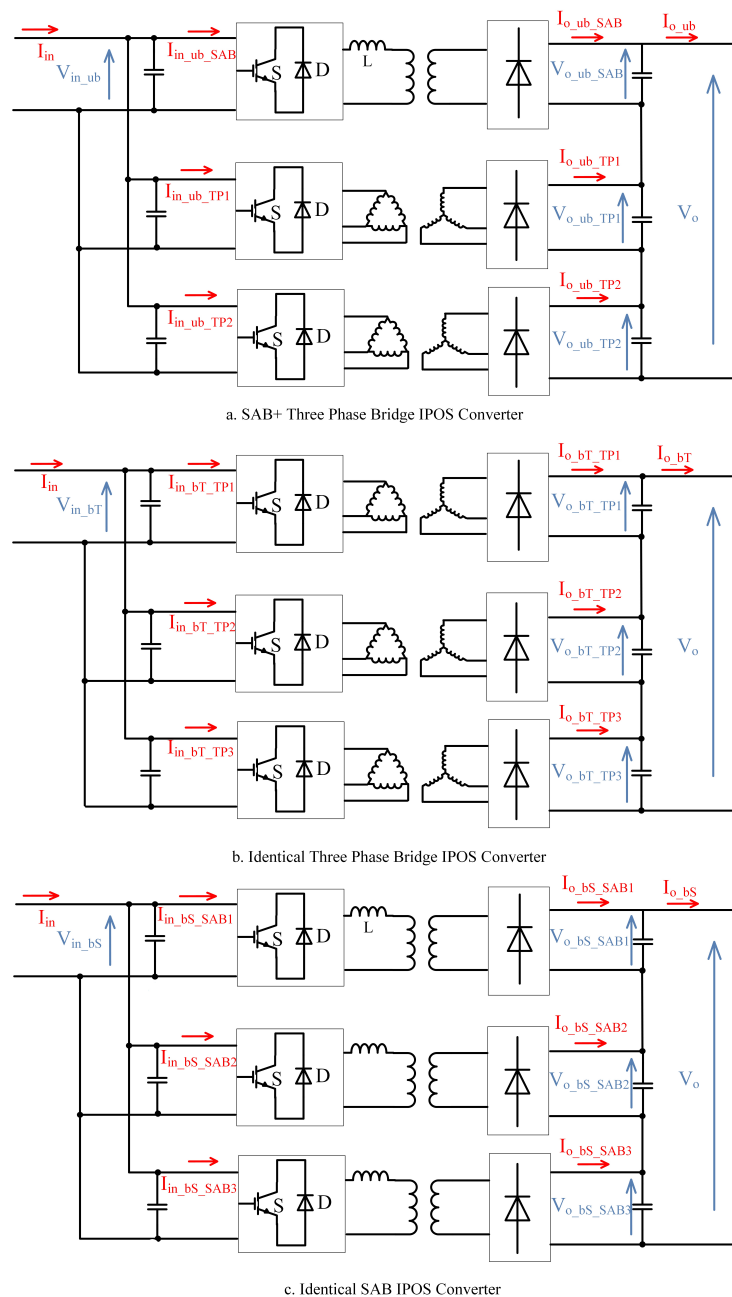


Figure 4. Three different unidirectional IPOS converter structures [8].

2.2. Asynchronous Characteristic among Multi-Connected 5MW SAB Converters

In an offshore wind farm, the distance between two adjacent 5 MW SAB converters is typically around 1 km due to the 5D principle. For these distances, it is very difficult to synchronise all the converters accurately, and small differences in frequency can cause large phase differences between different 5 MW SAB converters after a long operating time.

Instead of setting a long simulation time for the model, which is impractical, the following two different phase angle conditions with exactly synchronised 5 MW converters is studied. Thus, an extreme condition is applied in this study and the real performance of the system can be obtained by the calculation of the average value of data acquired from them.

1. All the switches of the three multi-connected 5 MW converters are controlled by the same signal;

2. There are 120 degree phase shifts between the switch control signals of the multi-connected 5 MW converters.

2.3. Phase Conditions of the Switch Control Signals of the Three Different IPOS Converters

In Figure 4, there are three different IPOS converter structures which can be used. For the unbalanced SAB + Three Phase IPOS structure and Identical Three Phase IPOS structure, an internal phase shift is not needed based on the characteristic of the Three Phase converter. For the Identical SAB IPOS converter structure, 120 degree phase shift signals are necessary for the switches of three IPOS connected SAB converters to limit the ripple content [9].

2.4. Definition of the Relative Losses

AC losses in the cable are caused by the current harmonics that vary for different frequencies. Based on the study in [10], it can be seen that higher frequency harmonic components can cause higher losses on the cables. Combining the results in [10], a new concept, relative losses (AC), is proposed to simplify the calculation.

Relative losses on the cables is a concept used in this research. It is based on the per unit method used widely in electrical power engineering. The unified base value is set for all terminal voltages and cable currents, shown in Table 1, with reference to Figure 2. In the table, the base value of all the terminal voltages are set to be their nominal voltage, while the base value of all the cable currents at the multi-connected section are set as the approximate value when the wind speed is 10.3 m/s, which is the ten-year average wind speed of the Hywind Scotland Pilot Park Project in the North-east of Scotland [11].

Table 1. Base V=value of terminal voltages and cable currents in system.

Parameter	$V_{dc1,2,3}, V_{in_IPOS}$	$I_{dc1}, I_{2,3}$	Wind Speed
Base Value	50 kV DC	63 A DC	10.3 m/s

After the selection of the base value, the FFT analysis is put into the simulation results and the percentage ratio between the peak value of the harmonics at different frequencies and the DC base value can be obtained. The definition of Relative Losses and their calculation method can be found in Appendix A, and the calculated results are given directly in the main content.

3. Simulation Study of the Relative AC Losses and Voltage Total Harmonic Distortion of the System

In this section, Total Relative AC Losses caused by the multi-connected cable currents and Total Harmonic Distortion (THD) of cable terminal voltages with different capacitor values are compared, and the results are analysed. In the simulation, four different capacitor values, 0.4 μ F, 4 μ F, 40 μ F and 400 μ F were applied for the output capacitors of each 5 MW SAB converter (C_o in Figure 3) and the three input capacitors of the 15 MW IPOS converter (input capacitors in Figure 4). Although a 400 μ F capacitor is not realistic in this high voltage high power system, it is still included in the simulation to identify the performance characteristics of the system. The different capacitances are chosen to span four orders of magnitude in order to give sufficient variation in capacitance.

3.1. System Operating Parameters

In the simulation model, the wind speed experience by each turbine is set to be 10.3 m/s, as shown in Table 1. The DC voltage at the onshore receiving end of the system is set at a constant 400 kV. All other parameters and the detailed control circuit of the system can be found in [9]. During the entire simulation, only the input and output capacitor values and the type of the IPOS converter is varied throughout each simulation.

3.2. Varying Tendency of the Voltage Total Harmonic Distortion

Figure 5–7 shows the THD of cable terminal voltages in Figure 2 with three different IPOS converters, respectively. In each of the three figures, the THD of V_{dc1} – V_{dc3} and V_{in_IPOS} at different capacitor values are shown in four separate subfigures. In each of the subfigures, the 5 MW SAB converter output capacitor value and the 15 MW IPOS converter input capacitor value are varied with four different orders of magnitude and the results of the system with different filter capacitor values can be summarised as follows:

1. Comparing the subfigures (a), (b) and (c) in Figure 5 or Figure 6 or Figure 7, the THD of V_{dc1} , V_{dc2} and V_{dc3} is dominated by the output capacitors of the 5 MW SAB converters; this is found in systems with any of the three types of IPOS converters, as the THD is decreasing apparently with the increase of the order of magnitude of output capacitors of the 5 MW SAB converters. The input capacitor value of the IPOS converters does not significantly affect the THD of V_{dc1} , V_{dc2} and V_{dc3} ;
2. The THD of V_{in_IPOS} decreases with the increase of both output capacitor values of the 5 MW SAB converters and the input capacitor values of the IPOS converters, in systems with any of the three types of IPOS converters, which can be seen in subfigure (d) in Figure 5–7;
3. The overall voltage THD is lowest in the system with Identical Three Phase IPOS converters.

In addition to voltage THD, the simulation also provides current harmonics and cable AC losses. Figure 8 shows the total relative AC losses on the multi-section cables of systems with three different types of IPOS converter structure. Each value of total relative AC loss in each subfigure is a sum of the relative AC losses caused by I_{dc1} , I_2 and I_3 in Figure 2 on the submarine cables they are flowing through. Similar to the terminal voltage THD, the overall relative cable losses can be limited effectively by the output capacitors of the 5 MW SAB converters, while the increase of the value of the input capacitors of the IPOS converter does not have a significant effect on the cable AC losses. Moreover, the system with the Identical Three Phase IPOS converter structure has the lowest relative cable AC losses.

Combining all the simulation results, the value of the 5 MW SAB converter output capacitor can be set to 40 μF or 4 μF , while the input capacitors of all three types of IPOS converters are set to 0.4 μF , which is a compromise between the value of the ripple content and size of the capacitor. Both the THD of the terminal voltages and the Total Relative AC Losses on the cables at these particular capacitor values are shown in Figure 9 and Table 2 to provide more detailed results and to allow comparison. In Figure 9, and Table 2, OC is the output capacitor of the 5 MW SAB converter; IC is the input capacitor of the IPOS converter.

The results in Figure 9 show that for systems with the SAB + Three Phase IPOS converter structure and the Identical Three Phase IPOS structure, 4 μF OC and 0.4 μF IC can limit the THD of all terminal voltages to within 2%, which satisfies the requirements of the maximum voltage THD limit on the cables [10]. For the system with the Identical SAB IPOS converter structure, the value of the filter capacitors needs to be increased further to limit the voltage THD.

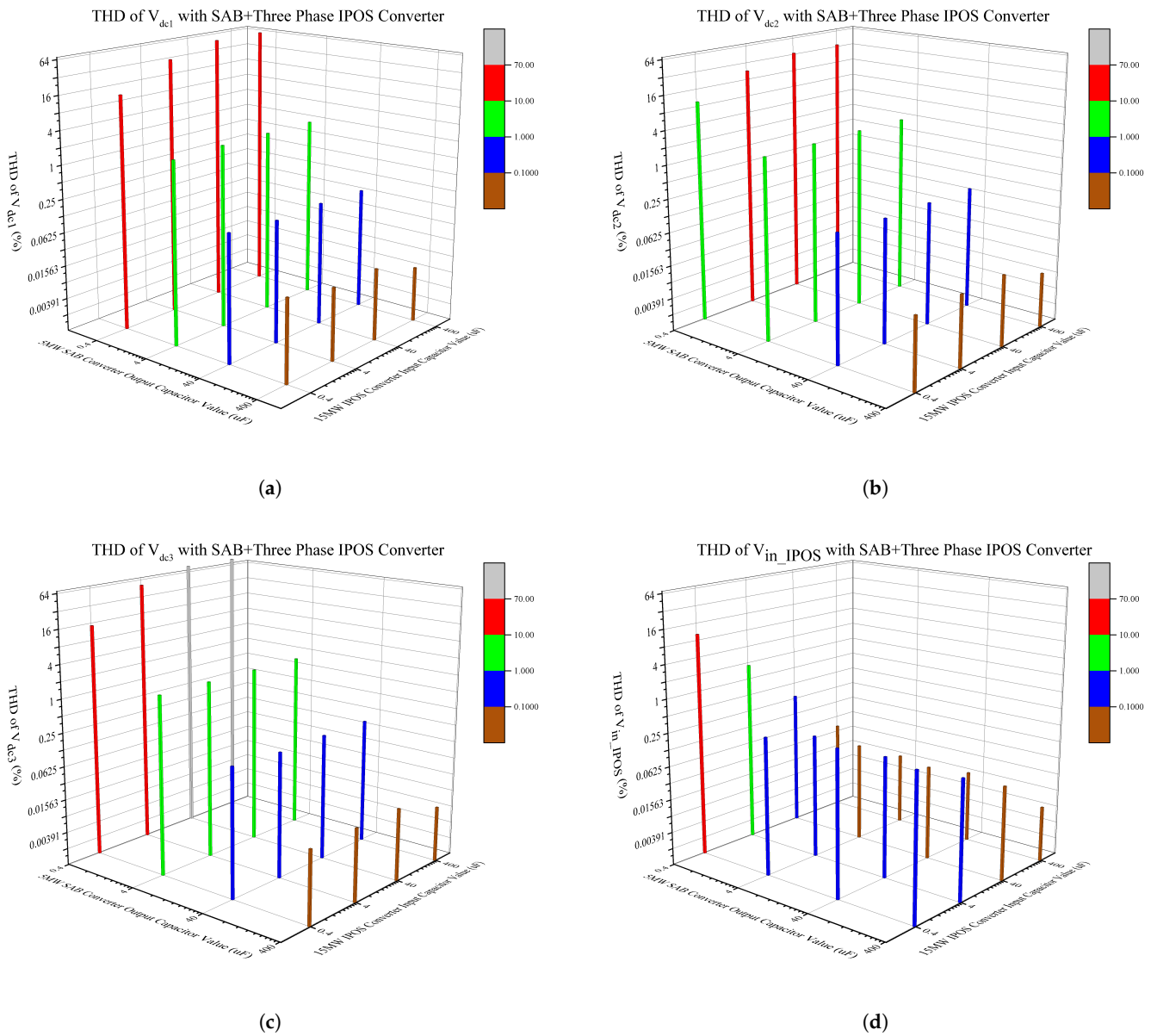


Figure 5. Total harmonic distortions of terminal voltages in Figure 2 in different filter capacitor values with SAB + Three Phase IPOS Converter. (a) Total harmonic distortions V_{dc1} ; (b) total harmonic distortions V_{dc2} ; (c) total harmonic distortions V_{dc3} ; and (d) total harmonic distortions V_{in_IPOS} .

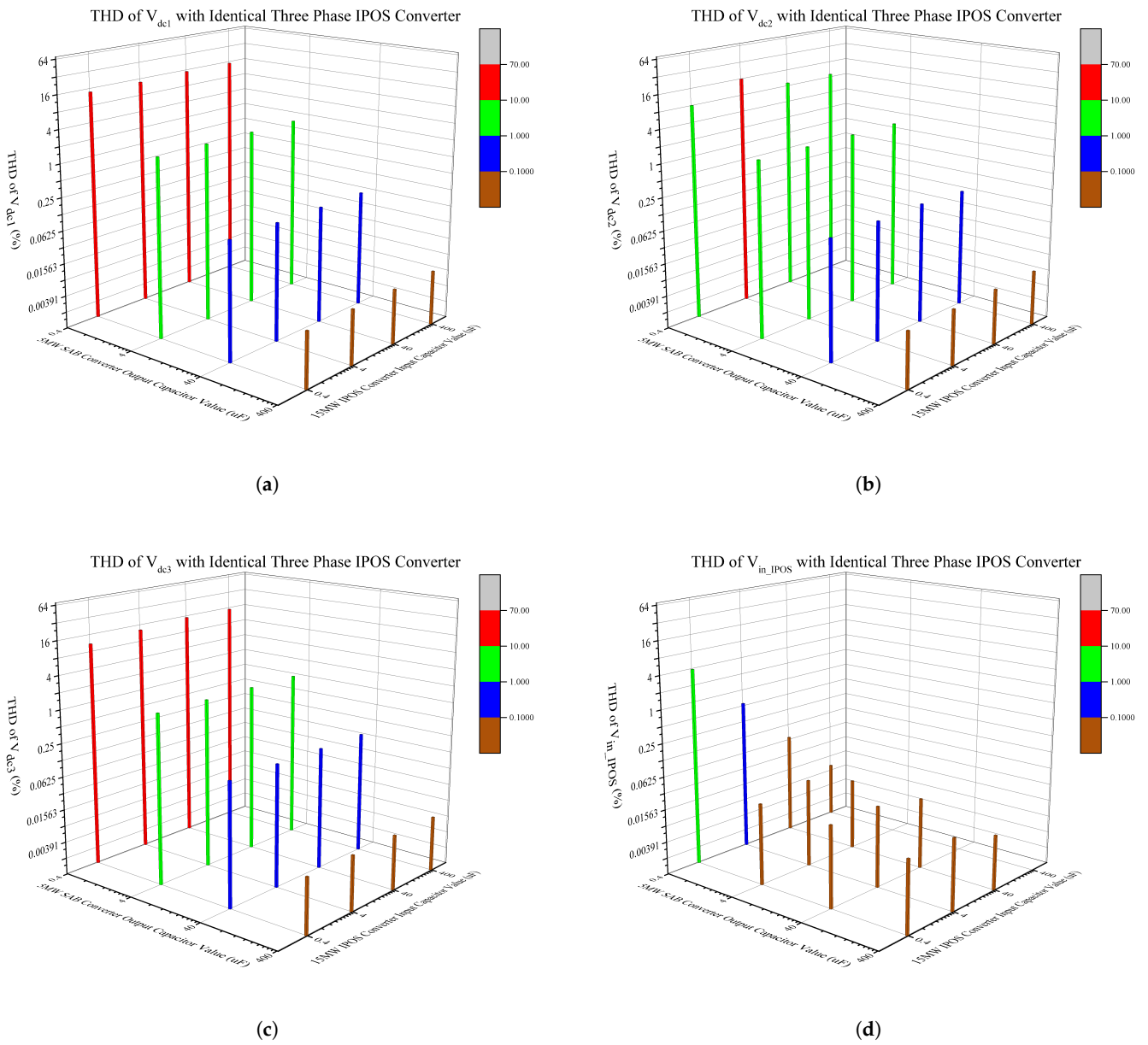


Figure 6. Total harmonic distortions of terminal voltages in Figure 2 in different filter capacitor values with Identical Three Phase IPOS Converter. (a) Total harmonic distortions V_{dc1} ; (b) total harmonic distortions V_{dc2} ; (c) total harmonic distortions V_{dc3} ; and (d) total harmonic distortions V_{in_IPOS} .

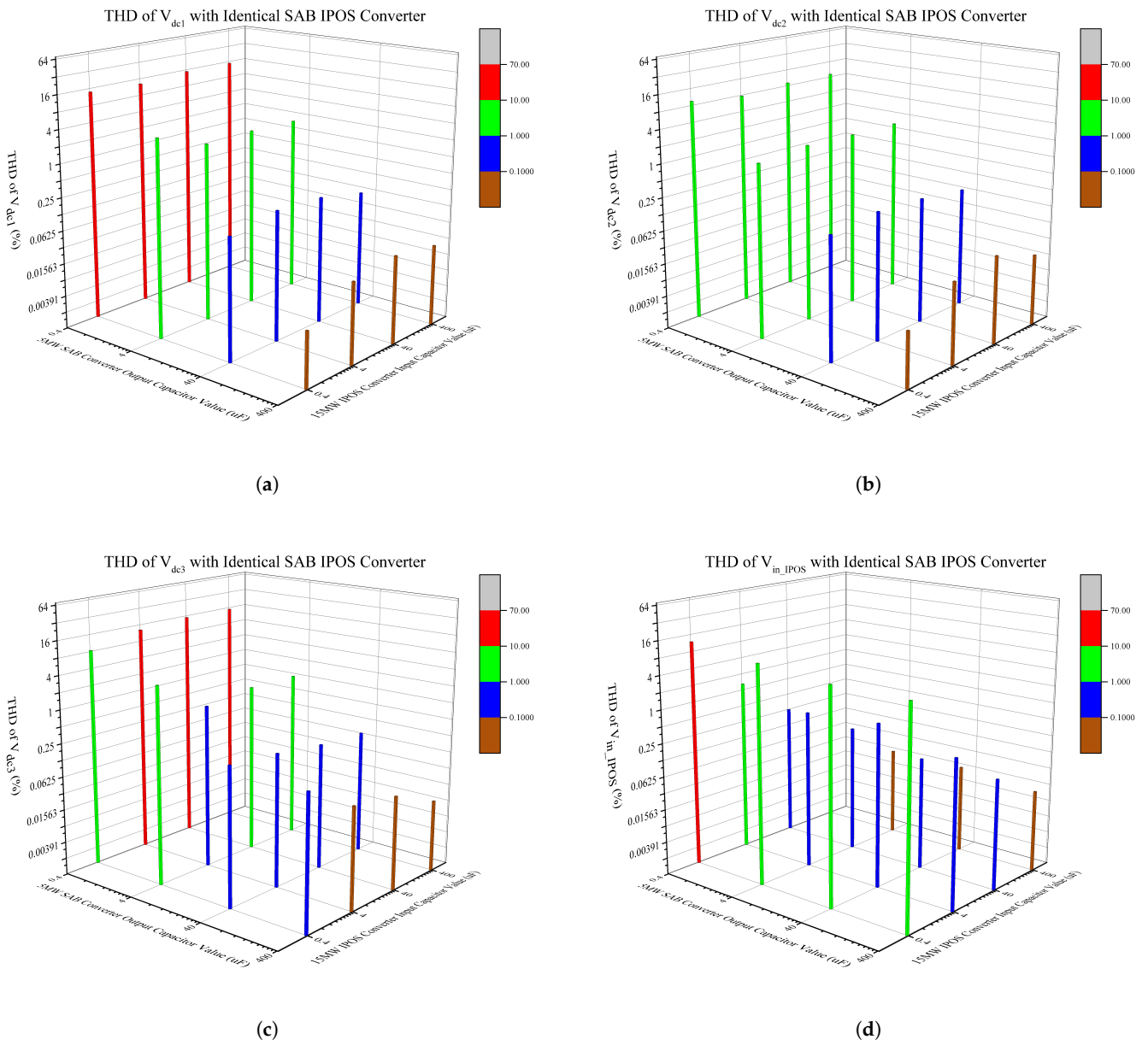


Figure 7. Total harmonic distortions of terminal voltages in Figure 2 in different filter capacitor values with identical SAB IPOS Converter. (a) Total harmonic distortions V_{dc1} ; (b) total harmonic distortions V_{dc2} ; (c) total harmonic distortions V_{dc3} ; and (d) total harmonic distortions V_{in_IPOS} .

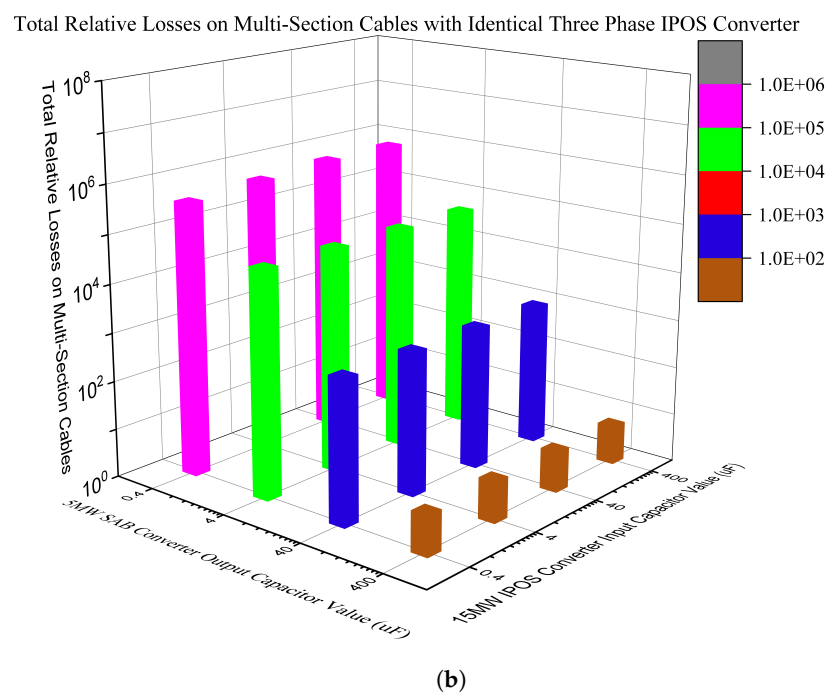
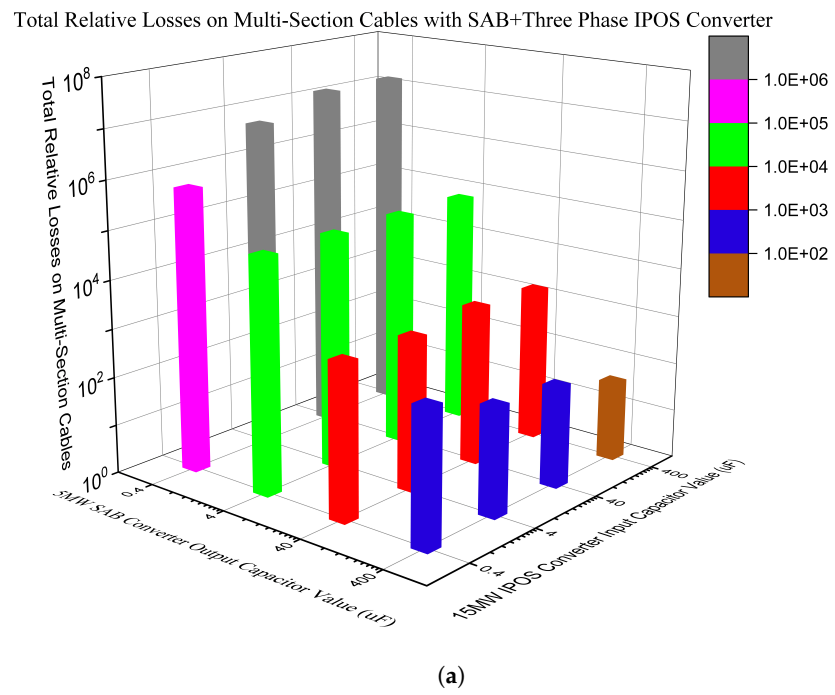


Figure 8. Cont.

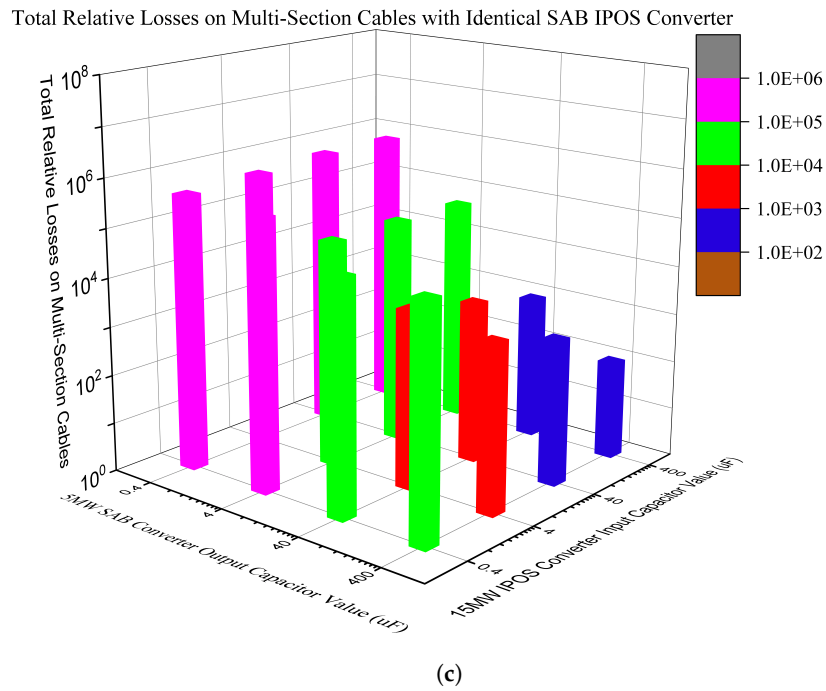


Figure 8. Total relative AC losses on multi-section cables with three different IPOS converter structures. (a) Total relative AC losses on multi-section cables with SAB+Three Phase IPOS Converter; (b) total relative AC losses on multi-section cables with identical Three Phase IPOS Converter; and (c) total relative AC losses on multi-section cables with Identical SAB IPOS Converter.

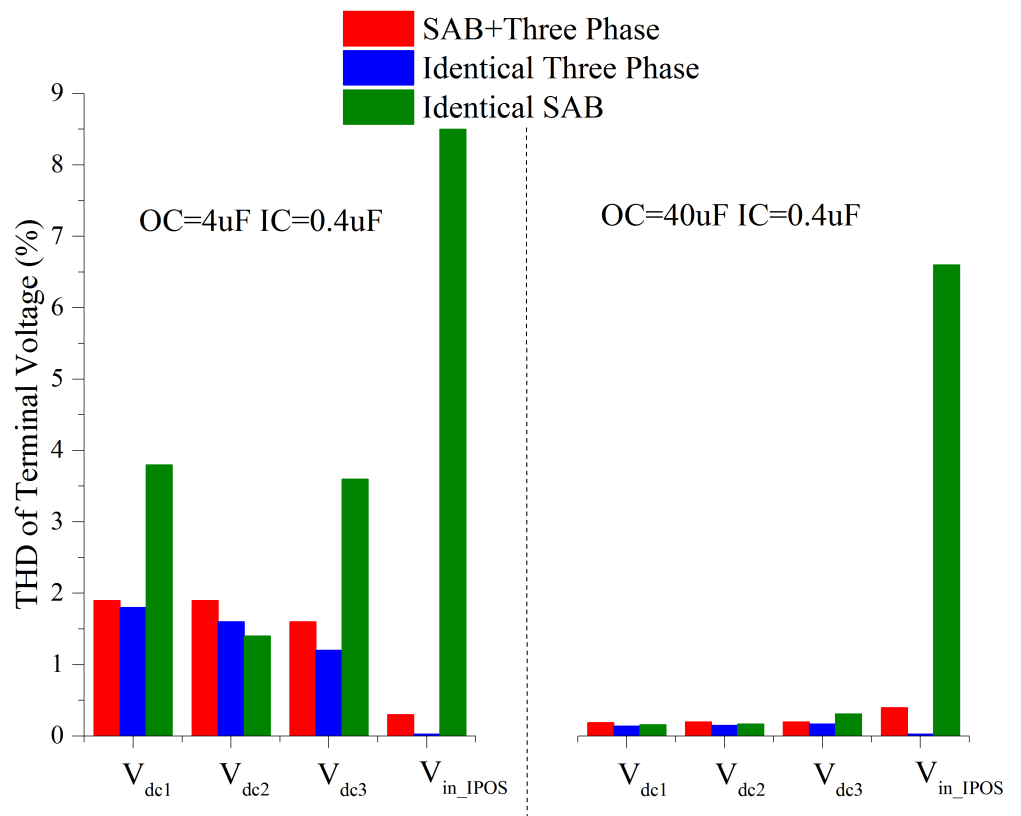


Figure 9. THD of terminal voltages at particular OC and IC.

Table 2. Total relative AC losses on multi-section cables with particular values of OC and IC.

Total Relative AC Losses on Multi-Section Cables with Particular Value of OC and IC					
OC = 4 μ F IC = 0.4 μ F			OC = 40 μ F IC = 0.4 μ F		
SAB + Three Phase	Identical Three Phase	Identical SAB	SAB + Three Phase	Identical Three Phase	Identical SAB
67 k	46 k	336 k	1.5 k	0.9 k	57 k

Regarding the total AC losses on the multi-section cables combined with the information in Table 1 and Figure A1, if looking at the OC = 4 μ F IC = 0.4 μ F part in Table 2 and putting values into Equation (A2), cable losses caused by the current harmonics, even with the Identical Three Phase IPOS converter structure, can reach:

$$\begin{aligned}
 & \text{Real Losses} \\
 & = 580 \times 10^{-3} \text{ W} \times (63 \text{ A} \times \%1)^2 \times 0.6 \text{ km} \times 2 \times 46 \times 10^3 \\
 & \approx 14 \text{ kW}
 \end{aligned}$$

14 kW is about 0.2% of the total power generated from the turbine at this steady state. Although 0.2% is not a large value, the high current ripple can affect the capacitor lifetime. Given the compromise between the value and physical size of the capacitors and the AC losses/current and voltage ripple content, the output capacitor value of the 5 MW SAB converter is suggested to be several tens of μ F for any of the three different types of IPOS converter structures. Table 3 summarises the final OC and IC values selected for systems with the three IPOS converter structures. A system with the Identical SAB IPOS converter needs to have a much bigger filter at the input of the IPOS converter to limit both terminal voltage ripple content and cable AC losses to a reasonable range. The system with the Identical Three Phase IPOS converter always has the best performance under the same filter condition.

Table 3. Filter selected for systems with different kinds of IPOS converter structure.

Capacitor	IPOS Converter Structure	SAB + Three Phase	Identical Three Phase	Identical SAB
	OC		40 μ F	40 μ F
IC		0.4 μ F	0.4 μ F	4 μ F

This study aims at giving a general understanding of the operation of the system, as well as selecting appropriate capacitor filters based on the voltage and current ripple content on the cables under different IPOS converter structures. The filter capacitor suggested in Table 3 can be applied in future studies of the system, while it needs to be noticed that, for example, 40 μ F would be a typical value rather than the required exact value.

4. Downscaled Hardware Testing of the Multi-Terminal DC System

In this section, a simplified and downscaled hardware model of the system shown in Figure 2 is built and tested, in order to verify the conclusion obtained from the simulation results, which describes the relationship between the ripple content and the terminal filters. Figure 10 shows a photograph of the downscaled multi-terminal DC system built in the laboratory. During the experiment, the input current of all the 5 W SAB DC-DC converter is set to be 1 A, and the voltage of the input power source can be adjusted according to the current and the characteristic of the system. The voltage value of the receiving end DC Battery is about 12.5 V.

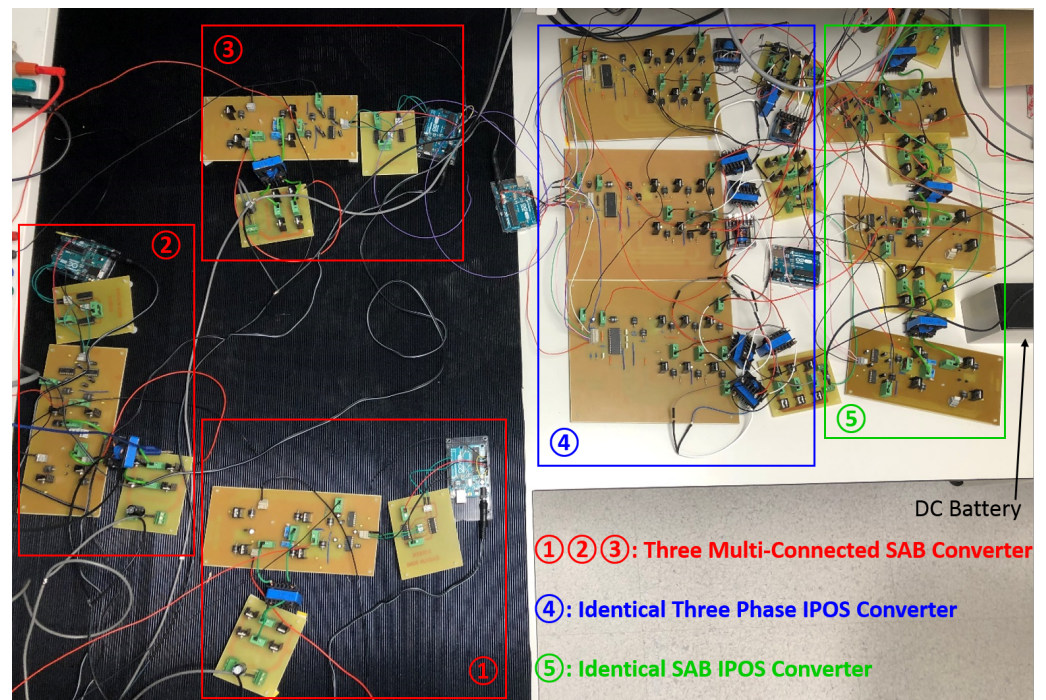


Figure 10. The prototype of the downscaled and simplified multi-terminal DC system.

The length of the multi-connected cable is selected to be 2 m in the experiment. Based on the study of the IPOS converter in [8], the switching frequencies of the converters in the downscaled model are about 30 times higher than that in the simulation model, so the length of the cable in the experiment should be selected as $600 \text{ m}/30 = 20 \text{ m}$. However, 20 m of cable at each section is not easily achieved, and can cause a significant voltage drop due to the low voltage level in the experiment. According to the status quo, the length of the cable is reduced further to 2 m, which will not affect the performance of the filter capacitors in the system when different results are compared.

In this downscaled experiment, two different capacitor values, $10 \mu\text{F}$ and $1000 \mu\text{F}$, are used for both three output capacitors (OC) of the three 5 W SAB converters and three input capacitors (IC) of the 15 W IPOS converter. The value of OC and IC are wax and wane. As for the structure of the IPOS converter, Identical Three Phase IPOS converter and Identical SAB IPOS converter are operated in the system separately and compared.

Figures 11–15 display the waveforms of V_{dc1} , V_{dc2} , V_{dc3} , V_{in_IPOS} , I_{dc1} , I_2 and I_3 with different filter capacitor values and IPOS converter structures. In these figures, all the terminal voltage values in the system with Identical Three Phase IPOS converter are slightly lower than those in the system with Identical SAB converter. It is because of the sum up of the V_o/V_{in} of each Three Phase converter in the IPOS converter structure is slightly higher than that of the IPOS structure with SAB converter. Under this circumstance, once the value of the DC battery is not changed, the input voltage of the Identical Three Phase IPOS converter can be slightly lower as well as all terminal voltages.

Comparing the two different waveforms in each subfigure in Figures 11–13, the ripple content of all the terminal voltages can be limited better once the higher capacitor value is applied for the output capacitor (OC) of the 5 W SAB converter. Moreover, from subfigure (a) and (b) in each figure of Figures 11–13, the system with Identical Three Phase IPOS converter can always have lower ripple content. These phenomena correspond to the conclusions obtained in the simulation model.

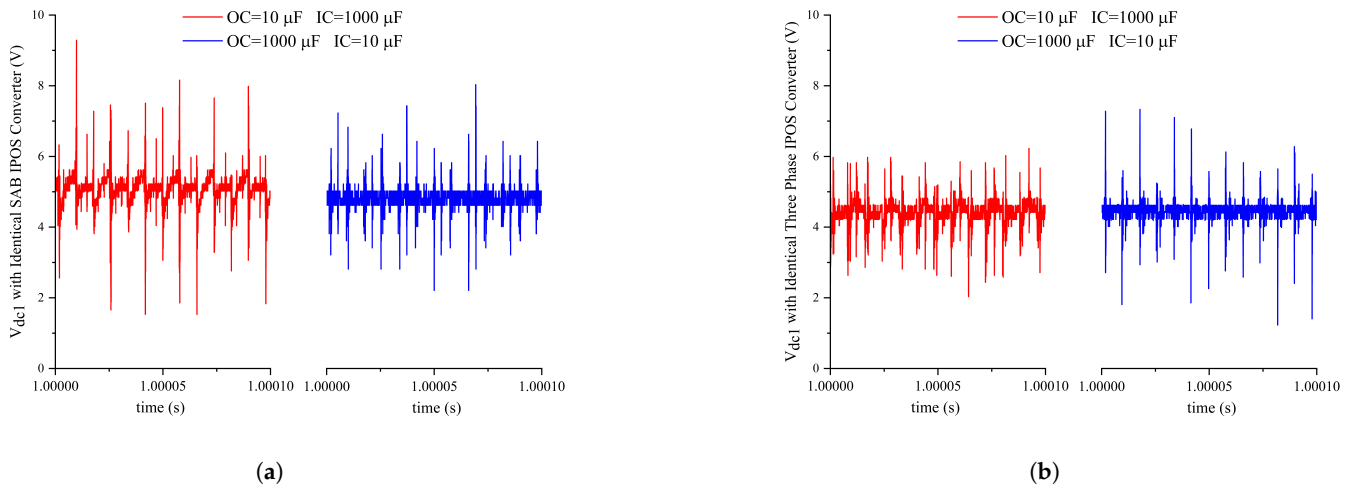


Figure 11. Comparison of the waveform of V_{dc1} under different situations. (a) V_{dc1} with Identical SAB IPOS Converter; and (b) V_{dc1} with Identical Three Phase IPOS Converter.

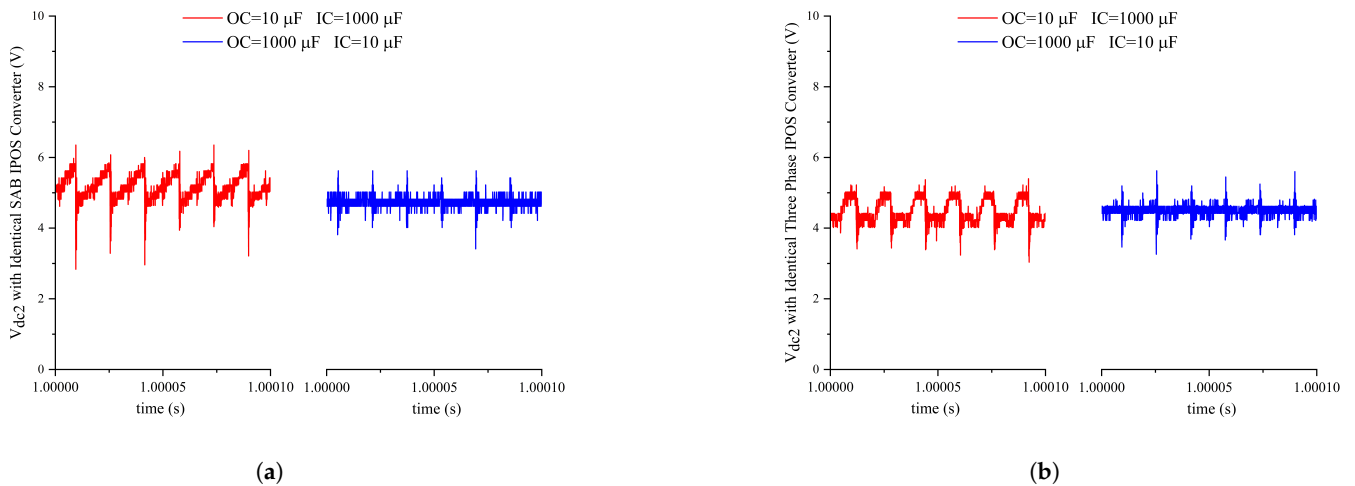


Figure 12. Comparison of the waveform of V_{dc2} under different situations. (a) V_{dc2} with Identical SAB IPOS Converter; and (b) V_{dc2} with Identical Three Phase IPOS Converter.

In Figure 14a,b, it can be seen that for the V_{in_IPOS} , the effect of the OC and IC are similar. This time, the advantages of the system with Identical Three Phase IPOS converter is not clear, which is because of the noise overlapping the ripple itself, as the V_{in_IPOS} has very low ripple content under all the cases during the test. It is also noted that the position of the probe can influence the noise during the test.

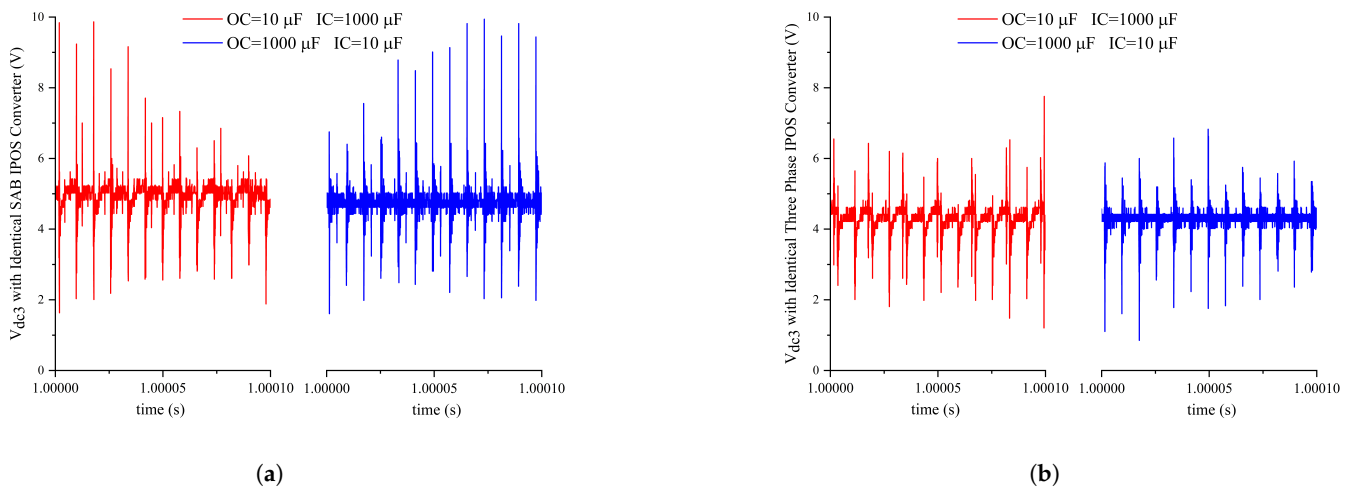


Figure 13. Comparison of the waveform of V_{dc3} under different situations. (a) V_{dc3} with Identical SAB IPOS Converter; and (b) V_{dc3} with Identical Three Phase IPOS Converter.

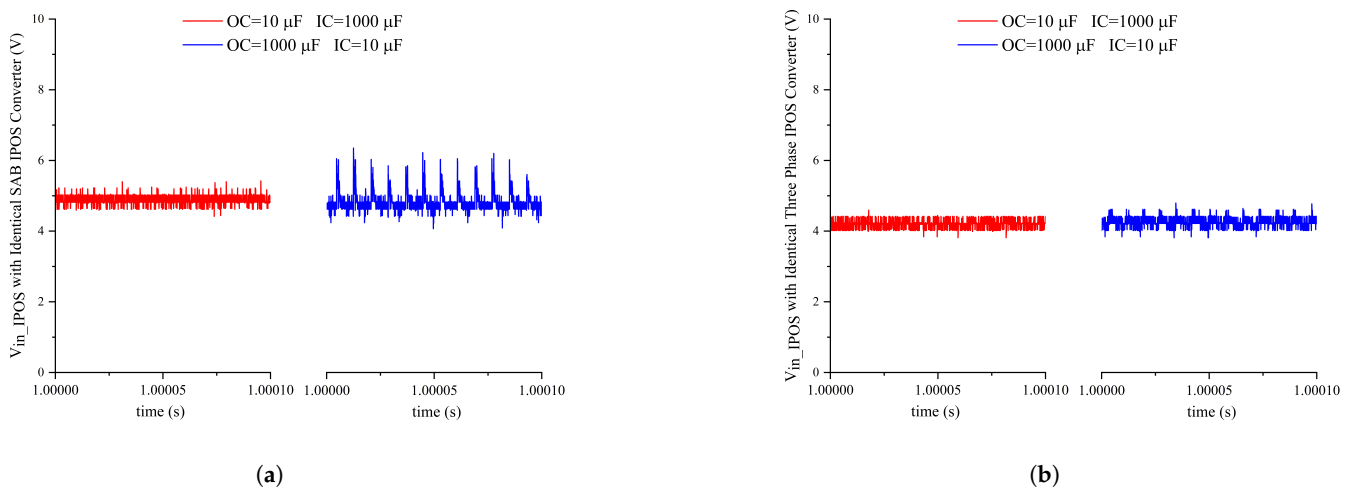


Figure 14. Comparison of the waveform of V_{in_IPOS} under different situations. (a) V_{in_IPOS} with Identical SAB IPOS Converter; and (b) V_{in_IPOS} with Identical Three Phase IPOS Converter.

Figure 15 displays the waveform of cable currents. The output current of each 5 W SAB converter feeds into the cables and flows into the IPOS converter. The peak to peak value of I_{dc1} in Figure 15a,b are similar, but if looking at the waveform of I_2 and I_3 , it is clear that their ripple content is higher in the system with Identical SAB IPOS converter, which means the system with Identical Three Phase IPOS converter has lower overall cable ripple content, and total relative losses. Furthermore, the ripple of the current with higher SAB converter output capacitor value is smaller in both Figure 15a,b, so the better effects of the output capacitors of the multi-connected SAB converters are apparent. This test result confirms the same conclusion as in the simulation work.

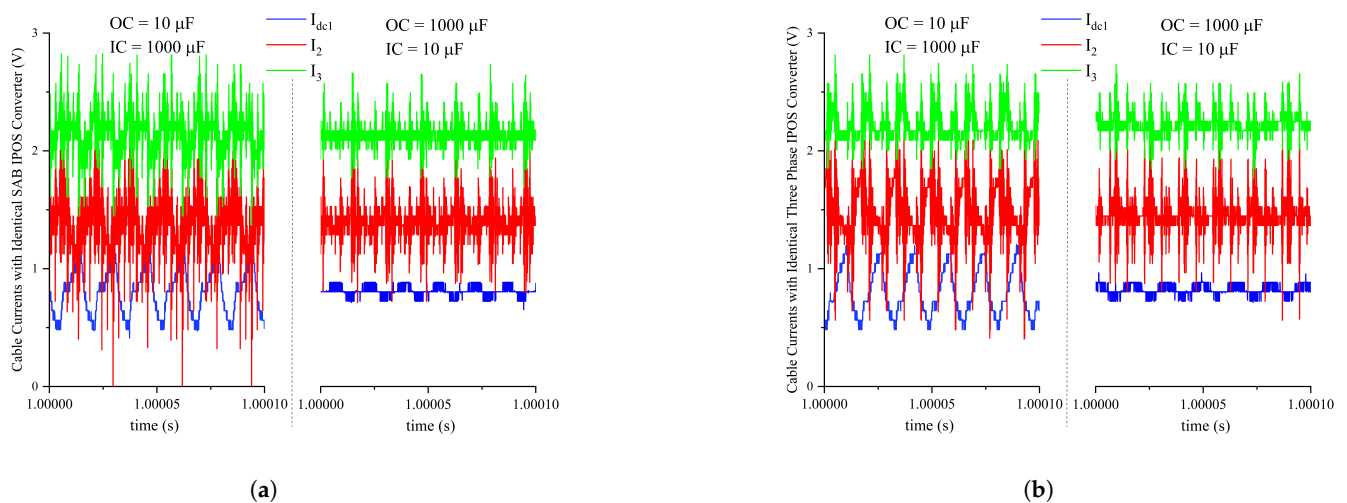


Figure 15. Comparison of the waveform of cable currents under different situations. (a) I_{dc1} , I_2 and I_3 with Identical SAB IPOS Converter; and (b) I_{dc1} , I_2 and I_3 with Identical Three Phase IPOS Converter.

5. Conclusions

Filters at the multi-connected section of the system, such as the output capacitor of the 5 MW SAB converter and the input capacitor of the IPOS/ISIPOS converter in this study, play a crucial role in the limitation of ripple content and losses in the multi-connected cables. From the case study in this paper, it can be seen that the output filter of the 5 MW converter plays a much more critical role in the reduction of both voltage ripple content and AC losses on the cables. Under this circumstance, the input filter value of the IPOS/ISIPOS converter can be much smaller than the output filter value of the 5 MW SAB converter, while the design of the latter should also be carried out carefully when building a real system.

The type of the IPOS converter applied in the system can also have significant influences on the THD of terminal voltages and cable AC losses. In this study, the advantages of the Three Phase DC-DC converter applied for the IPOS converter structure are visible in both simulation and hardware tests.

Author Contributions: Conceptualization, X.R. and D.E.M.; methodology, X.R.; software, X.R.; validation, X.R., J.K.H.S. and D.E.M.; formal analysis, X.R. and D.E.M.; investigation, X.R., J.K.H.S. and D.E.M.; resources, X.R. and P.M.; data curation, X.R.; writing—original draft preparation, X.R.; writing—review and editing, X.R., J.K.H.S. and D.E.M.; visualization, X.R., J.K.H.S. and D.E.M.; supervision, J.K.H.S., D.E.M. and P.M.; project administration, D.E.M. All authors have read and agreed to the published version of the manuscript.

Funding: This research received no external funding.

Institutional Review Board Statement: Not applicable.

Informed Consent Statement: Not applicable.

Data Availability Statement: Data sharing not applicable. No new data were created or analysed in this study. Data sharing is not applicable to this article.

Acknowledgments: The authors would like to thank the Edinburgh University school of Engineering technical staff Kevin Tierney, Douglas Carmichael, Iain Gold, Jamie Graham, Alasdair Christie for their help on making PCBs and giving technical guidance in this research.

Conflicts of Interest: The authors declare no conflict of interest.

Appendix A. Definition and Calculation Method of Relative AC Losses on Cables

This work is concentrated on the study of the AC losses on the submarine cables of the offshore wind farm based multi-terminal DC link under different capacitor situations.

If all the calculations are based on the real losses, tedious fraction numbers can be involved throughout the paper. Inspired by the definition of the per unit, a new concept, relative losses, is used to sweep aside tedious fractions and has conspicuous advantages.

One detailed and comprehensive study of the losses on DC cables in the similar multi-terminal DC system can be found in [10]. Taking these research results as the reference and with some reasonable approximations, Figure A1 can be concluded to show the Characteristic of the AC Losses on the 50 kV or ± 25 kV cable in Figure 2.

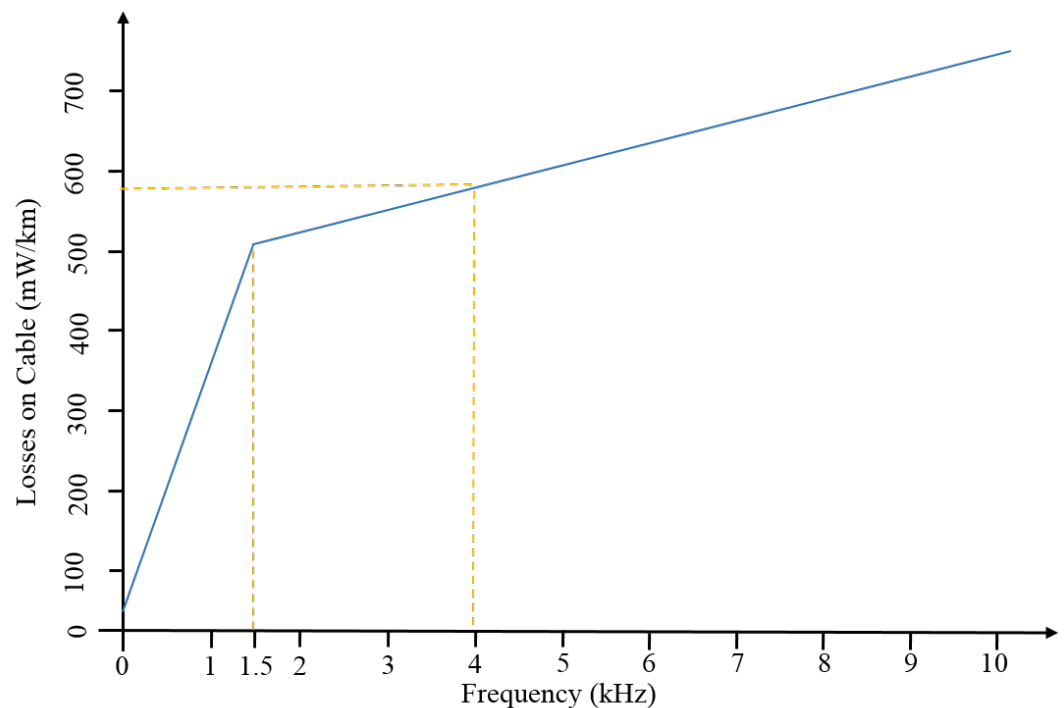


Figure A1. Cable losses at a range of frequencies with AC current magnitude of 1A at each frequency [10].

The DC losses on the cable can also be studied based on the figure; few previous studies focus on the cable AC losses in a DC system. In this research, all the losses studied are on the AC losses of the submarine cables in the system. However, from Figure A1, it can be identified that the DC losses are much lower than the AC losses caused by AC ripples, and sometimes can be disregarded.

According to Figure A1, if the loss on the cable caused by 4 kHz harmonic is set to be 1, the AC losses caused by ripples with different frequencies but the same magnitude can be identified in Equation (A1).

$$RL = \begin{cases} 1 + \frac{f-4}{4} \times 0.2 & f \geq 1.5 \\ 0.06 + \frac{f}{1.5} \times 0.815 & 0 \leq f < 1.5 \end{cases} \quad (\text{A1})$$

In Equation (A1), RL means the relative losses, and f is the frequency of the ripple having units (kHz). By applying the concept of the relative losses in the thesis, during the calculation, the real losses do not need to be taken into consideration, as well as the cable length. For example, if the total AC losses on three different cables need to be obtained, the relative losses on each of them can be calculated first and added up, before the multiplication with the correction number to acquire the final real value.

Assuming the current I_{dc1} has the ripple content in Table A1, the calculation procedure of the relative AC losses can be shown as below. In Table A1, the peak value of the

harmonics at dominate frequencies are represented as the percentage value relative to the specific base. If defining the losses caused by the 4 kHz ripple with 1% peak value of the base is 1, the Relative Losses caused by ripples of I_{dc1} at these four dominate frequencies can be calculated as:

$$\begin{aligned} & \text{Relative Losses Caused by Dominate Frequencies} \\ & = 100.9^2 + 32.5^2 \times 1.2 + 0.25^2 \times 1.4 + 0.48^2 \times 1.6 \end{aligned}$$

Table A1. Example relationship between the peak value of current ripple at different frequencies and base value.

Frequency	4 kHz	8 kHz	12 kHz	16 kHz
$I_{dc1_ripple_peak}:I_{dc_base}(\%)$	100.9	32.5	0.25	0.48

Relative AC losses happened at any frequencies can be calculated with the same method as shown above and added up to identify the total relative losses under the specific definition. One thing need to be mentioned here is in this study, ripple content with frequencies higher than 21 kHz are fall on deaf ears as their magnitudes are much smaller than that of the ripples on dominate frequencies, so sweeping them aside is a reasonable approximation. When the real AC losses need to be obtained, based on the particular situation, by the multiplication with the corresponding correction parameters, which can be acquired from the length and characteristics of the cable, real AC losses caused by ripples with 1 A amplitude in Figure A1, etc., the real AC losses can be derived easily, as illustrated in Equation (A2).

$$P_{RL} = P_{4Base} \times (I_{base} \times 1\%)^2 \times L_{cable} \times 2 \times TRL \quad (A2)$$

where P_{RL} is the real AC losses caused by harmonics on cables, P_{4Base} is the real losses caused by 4 kHz harmonic with 1 A amplitude on 1 km specific cable applied in the system, I_{base} is the base value selected when calculating the relative AC losses, L_{cable} is the length the submarine cable, 2 is an integer which indicates the onward and returned submarine cables, TRL is the total relative AC losses defined in this thesis and caused by harmonics at different frequencies.

References

1. Kwon, G.Y. Offline Fault Localization Technique on HVDC Submarine Cable via Time-Frequency Domain Reflectometry. *IEEE Trans. Power Deliv.* **2017**, *3*, 1626–1635. [[CrossRef](#)]
2. Liu, C.; Lai, J.S. Low frequency current ripple reduction technique with active control in a fuel cell power system with inverter load. *IEEE Trans. Power Electron.* **2007**, *4*, 1429–1436. [[CrossRef](#)]
3. Lee, W.J.; Sul, S.K. DC-Link Voltage Stabilization for Reduced DC-Link Capacitor Inverter. *IEEE Trans. Ind. Appl.* **2014**, *1*, 404–414.
4. Li, X.; Li, Z.; Zhao, B.; Lu, C.; Song, Q.; Zhou, Y.; Rao, H.; Xu, S.; Zhu, Z. HVdc Reactor Reduction Method Based on Virtual Reactor Fault Current Limiting Control of MMC. *IEEE Trans. Ind. Electron.* **2020**, *12*, 9991–10000. [[CrossRef](#)]
5. Liu, Z.; Zhao, J. Disturbance Interaction Analysis and Suppression Strategy of MMC-HVDC Systems Considering Sub-Module Capacitor Voltage Ripples. *IEEE Trans. Power Syst.* **2021**, *1*, 235–247. [[CrossRef](#)]
6. Lin, S.; Mu, D.; Liu, L.; Lei, Y.; Dong, X. A Novel Fault Diagnosis Method for DC Filter in HVDC Systems Based on Parameter Identification. *IEEE Trans. Instrum. Meas.* **2020**, *9*, 5969–5971. [[CrossRef](#)]
7. Xue, Y.; Zhang, X.; Yang, C. Series Capacitor Compensated AC Filterless Flexible LCC HVDC With Enhanced Power Transfer Under Unbalanced Faults. *IEEE Trans. Power Syst.* **2019**, *4*, 3069–3080. [[CrossRef](#)]
8. Rong, X.; Shek, J.K.H.; Macpherson, D.E. The study of different unidirectional input parallel output series connected DC-DC converters for wind farm based multi-connected DC system. *Int. Trans. Electr. Energy Syst.* **2021**, *5*, 1–16.
9. Rong, X. The Study of the Offshore Wind Farm Based Multi-Terminal DC System and the Application of High Power DC-DC Converters. Ph.D. Thesis, University of Edinburgh, Edinburgh, UK, 2018.

-
10. Wood, T. Interaction of DC-DC Converters and Submarine Power Cables in Offshore Wind Farm DC Network. Ph.D. Thesis, University of Edinburgh, Edinburgh, UK, 2013.
 11. 4C-Offshore. Hywind Scotland Pilot Park Offshore Wind Farm. Available online: <http://www.4coffshore.com/windfarms/hywind-scotland-pilot-park-united-kingdom-uk76.html> (accessed on 5 June 2017).